



Effect of Reaction Time and Precursor Concentration in the Structural Properties of TiO₂ Nanoparticles Synthesized by Low Temperature Sol-Gel Method

B.Gomathi Thanga Keerthana, P. Murugakoothan*

MRDL, PG and Research Department of Physics, Pachaiyappa's College, Chennai 600 030, India.

Abstract : Titanium dioxide (TiO₂) nanoparticles were synthesized by sol-gel method at low temperature using different precursor concentrations and reaction times. The synthesized samples were calcined at 400°C. The phase formation of titanium dioxide was identified from powder X-ray diffraction study. Lattice strain was found using Williamson-Hall (W-H) analysis. SEM images revealed the spherical shape of the TiO₂ nanoparticles. The presence of functional groups in TiO₂ nanoparticles were identified using FTIR analysis. UV-vis diffuse reflectance spectral study was used to determine bandgap of the samples. The luminescent property of the synthesized material was found to have its emission wavelength in the UV-region assessed by photoluminescence study.

Keywords : Sol-Gel method, TiO₂, SEM, W-H analysis.

Introduction

Titanium dioxide (TiO₂) is the most preferred photocatalyst considering its relatively high efficiency, chemical stability, photostability, non-toxicity and low cost. Among the semi-conducting oxides, TiO₂ is of great interest due to its outstanding physiochemical properties and increasing demand for functional devices with elevated properties [1]. Characteristically, titania exists in three crystal forms, such as anatase, brookite and rutile. Anatase is considered to be the most photoactive phase, whereas, rutile, the most thermodynamically stable form and pure brookite is very difficult to prepare. The heat treatment of nanoparticles plays a vital role in the synthesis, morphology, crystallinity and porosity and causing a decline in surface area, loss of surface hydroxyl groups and inducing phase transformation. At high temperatures say 400°C and above organic materials are most probably removed [2]. Due to calcination time and heating rate, the surface area of TiO₂ decreases, which in turn collapses the pores in the TiO₂ powder which may be caused by the phase transformation of amorphous TiO₂ to the anatase phase of TiO₂. Heating samples above 400°C results in good crystallinity of TiO₂ and this is considered as the most common method to produce TiO₂ material with good photocatalytic properties [3]. Researchers have synthesized TiO₂ nanostructures by several techniques like sol-gel, hydrothermal, solvothermal, electro-deposition method etc. Over a period of time, sol-gel method has emerged as a commonly used method for the preparation of TiO₂ nanocrystals [4]. Sol-gel is a solution based method wherein material structure is created by chemical reactions in liquid state and nanostructure materials can be formed with controlled shape in the form of powder or films [5]. Herein, we have reported the synthesis of anatase and brookite mixed phase of TiO₂ particles via sol-gel method at low temperature using different precursor concentrations and reaction times. Reaction time and pre-cursor ratio are applied as the experimental parameters, and their resulting influence are studied in this present work. Moreover the experimental parameters of the present work have been compared with the existing literature.

Experimental procedure

Materials

Tetrabutyltitanate($C_{16}H_{36}O_4Ti$) was purchased fromSigma Aldrich. Nitric acid and ethanol were purchased from Merck and de-ionized water was used throughout the experiments.

Synthesis

Tetrabutyltitanate was actuated as precursor, ethanol as the solvent, nitric acid as the catalyst and water for hydrolysis. Various amounts of nitric acid(0.5 mL, 1 mL and 1.5 mL) were added dropwise into 30 mL of ethanol under effective stirring. While stirring, different concentrations of tetrabutyltitanate (9 mL and 9.5 mL) were slowly added to the solution and left for 30 minutes. The acquired mixture was pale yellow in colour. Then the resulting yellow colour mixture was slowly added to 70 mL of distilled water at room temperature and kept under vigorous stirring for 30 minutes. The obtained solution was heated at 70°C using a magnetic stirrer employed with a hot plate for different time durations (6h, 8h and 10 h) to form gel. After the gelation, the wet gels were washed with distilled water and ethanol and dried at 80°C. Finally, the obtained micro granules were grounded and calcined at 400°C using a muffle furnace for 2 hours. The synthesized samples were named as S1, S2 and S3 and their experimental parameters are given in Table1.

Table 1 :Sample code with experimental parameters and also comparison results with existing literature

| Sample code | Temperature (°C) | Reaction Time (h) | Calcination (°C) | Precursor concentration | | Particle size | [Ref.] |
|-------------|------------------|-------------------|------------------|--------------------------|------------------|------------------------|--------------|
| | | | | Tetrabutyl titanate (mL) | Nitric acid (mL) | | |
| S1 | 70 | 6h | 400 | 9 | 1 | $0.74 \pm 0.02 \mu m$ | Present work |
| S2 | 70 | 8h | 400 | 9.5 | 1.5 | $0.77 \pm 0.01 \mu m$ | |
| S3 | 70 | 10h | 400 | 9.5 | 1 | $0.82 \pm 0.021 \mu m$ | |
| S1 | 50 | 12 | --- | 9.75 | 0.1 | 6.76 nm | [6] |
| S2 | 50 | 12 | --- | 19.5 | 0.1 | 6.13 nm | |
| S3 | 50 | 6 | --- | 9.75 | 0.05 | 6.58 nm | |
| S4 | 50 | 12 | --- | 9.75 | 0.05 | 6.64 nm | |

Characterization

The synthesized TiO_2 nanoparticles were characterized by X-ray diffraction for phase formation analysis using PANalytical X'PertPro diffractometer employing $CuK\alpha$ radiation ($\lambda=1.5406 \text{ \AA}$). The chemical structure was investigated by AVATAR 330 Fourier transform infrared spectrometer (FTIR) in which the IR spectrum was recorded by diluting the milled powder in KBr in the region between 4000 and 400 cm^{-1} . Diffuse reflectance spectrum of TiO_2 nanoparticles was recorded in the wavelength range from 190 nm to 900 nm in the diffused reflectance spectrum (DRS) mode with $BaSO_4$ as a reference material using LABINDIA Model UV 3092 spectrophotometer. Morphological study was done by scanning electron microscope (SEM) using JEOL Model JSM 6390LV. Photoluminescence (PL) study was carried out using Cary Eclipse Spectrophotometer with a 450W Xenon arc lamp as an excitation source.

Results and discussion

X-ray diffraction study

The PXRD patterns of calcined TiO₂ powders (samples S1,S2 andS3) at 400⁰C for 2h are shown in Figure 1. These results show that all the samples display the characteristic peaks of anatase and brookite. Most of the peaks belong to anatasephase and some of them correspond to brookite phase because of the variation in precursor concentration and reaction time [6].From the PXRD patterns, the 2θ values of the given peaks located at 25.1°, 37.5°,47.8°, 54.5°,62.5° and 75.1°are assigned to (101),(004),(200), (211), (204),(215)planes of anatase phase of TiO₂.The peaks located at 30.5°,37.5°,47.8°,54.5°and 63.2°are assigned to (121),(201),(231),(320),(312) planes of brookite phase of TiO₂. The presence of anatase phase was confirmed using the JCPDS files of #89-4203 and 89-8304and brookitephase was identified according to the JCPDS file #29-1360.

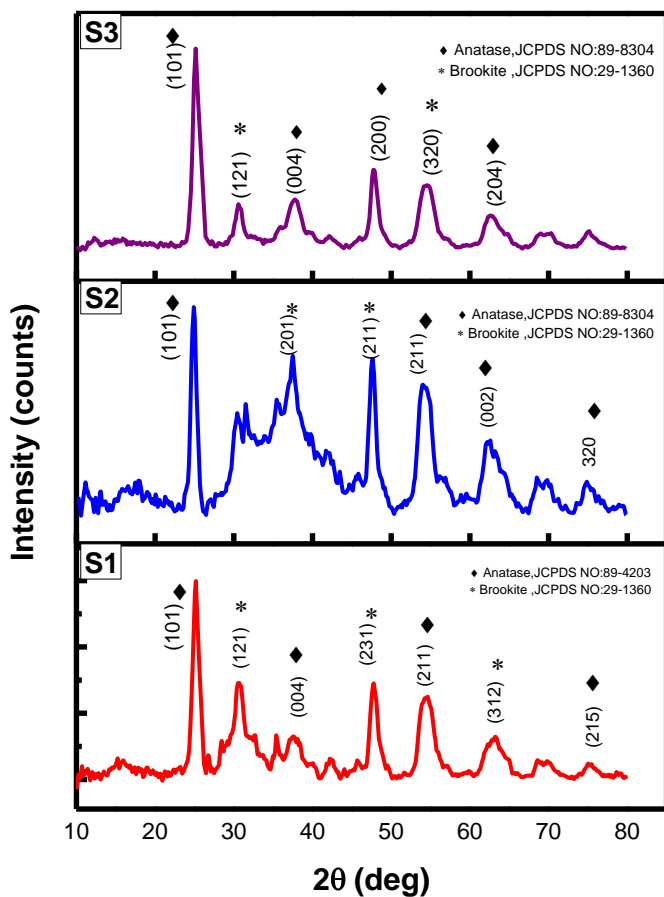


Fig 1 XRD patterns of TiO₂ samples S1,S2 and S3

Williamson-Hall analysis

By exploiting Williamson and Hall analysis, the size and strain broadening can be ascertained by looking at the peak width as a function of 2θ [7].It revealed that the defects present on the grain boundary produce lattice strain and prevent the grain growth and therefore, to confirm this statement, the lattice strain is resolved for each sample by acquiring the Williamson-Hall (W-H)equation as given below,

$$\beta_{hkl} \cos\theta = \frac{k\lambda}{D} + 4\epsilon \sin\theta$$

Where λ is the wavelength of X-ray radiation, β and θ are the full width half maximum (FWHM) and diffraction angle of the intense peaks respectively, D is the effective crystallitesize considering lattice strain and ε is the

effective value of lattice strain. The plot is drawn with $4\sin\theta$ on the X- axis and $\beta\cos\theta$ on the Y- axis (in radians).The particle size and strain are calculated from the intercept and slope obtained from linear fit of the data as shown in Figure 2 (a-c).The strain of as prepared nanoparticles was found to be -8.8×10^{-3} , -8.6×10^{-3} and -8.8×10^{-3} for samples S1, S2 and S3 respectively. The presence of negative strain indicates that the system is under compressive strain. As the crystallite size increases, the defects are gradually withdrew when the sample is subjected to heat treatment. Removal of grain boundary defects and increase of crystallite size reduces the stress field in the region, resulting in the release of lattice strain [8].Thus the increase of reaction time and calcination temperature would reduce the defects as well as increase the crystallite size and exhibit lower lattice strain.

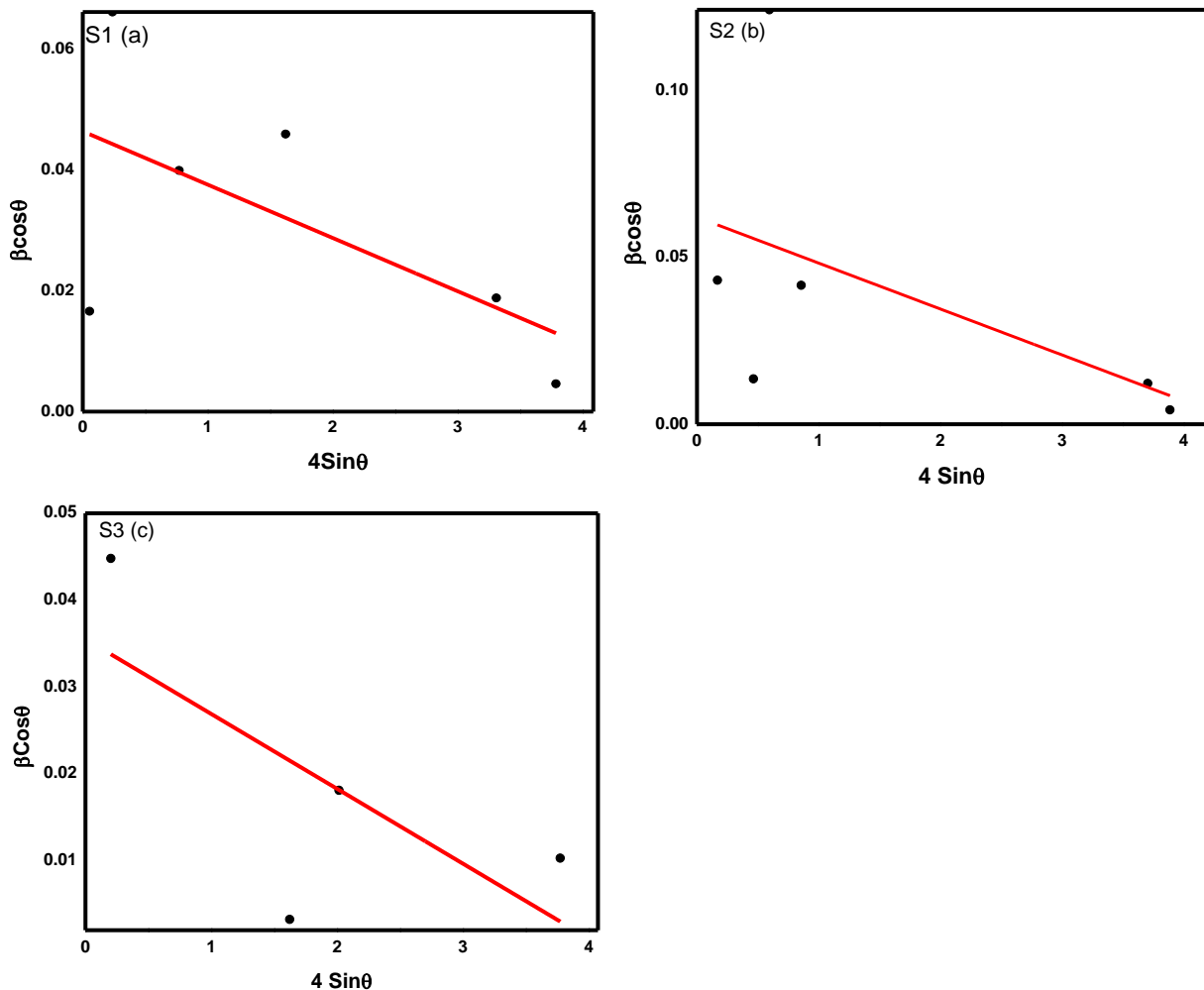


Fig2W-H plot of TiO₂ nanoparticles S1,S2 and S3

FTIR analysis

The FTIR study of nanoparticles shows the characteristics of the formation of high purity sample and depicts the functional groups of TiO₂ [10].The obtained FTIR spectra are shown in Figures 3 (a-c). FTIR results clearly revealed that the broad peak appearing between 3200 and 3600 cm^{-1} is assigned to the stretching vibration of O-H molecules coordinately adsorbed on the surface of Ti^{4+} ions and the small peak centered at 1618 cm^{-1} was due to bending vibrations of the surface-adsorbed water molecules[9-11]. This confirms the presence of hydroxyl group in the TiO₂nanoparticles. In the FTIR spectra, the presence of titania was confirmed from the peaks observed in the region between 800 - 450 cm^{-1} . It confirms the absence of organic residues in all the samples and are well matched with the already reported articles [11,12].

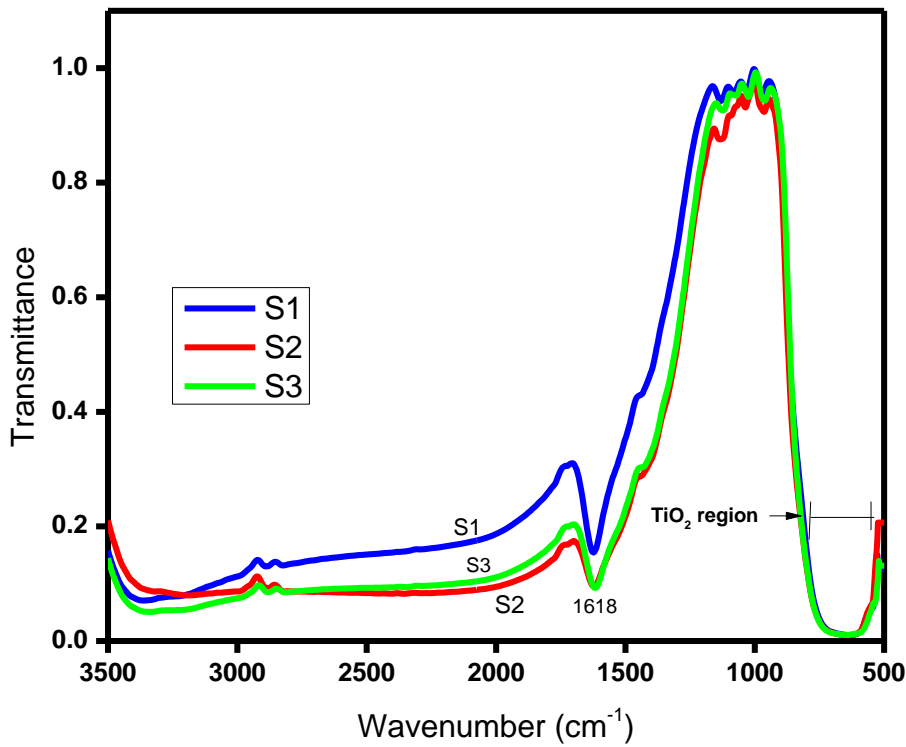
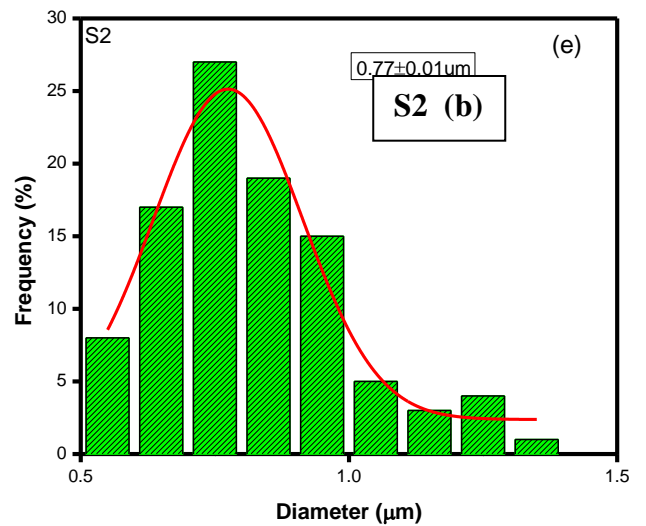
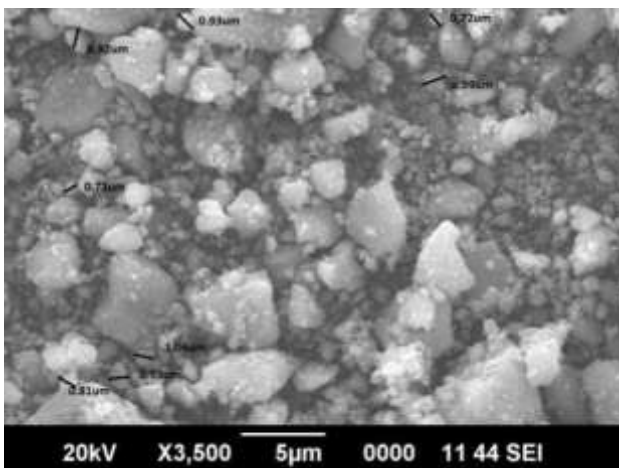
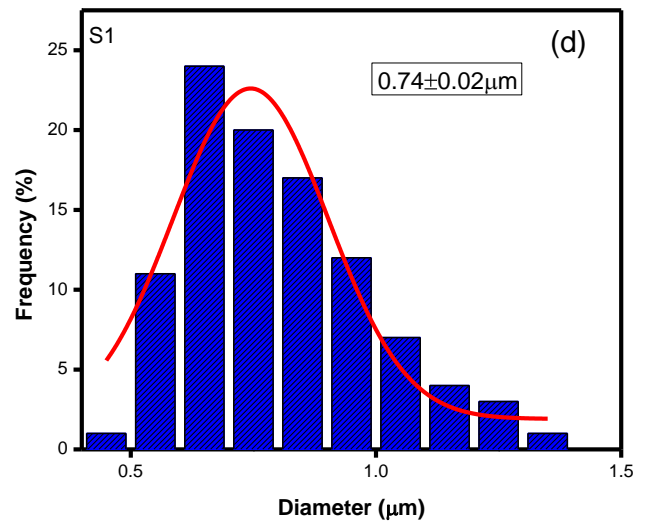
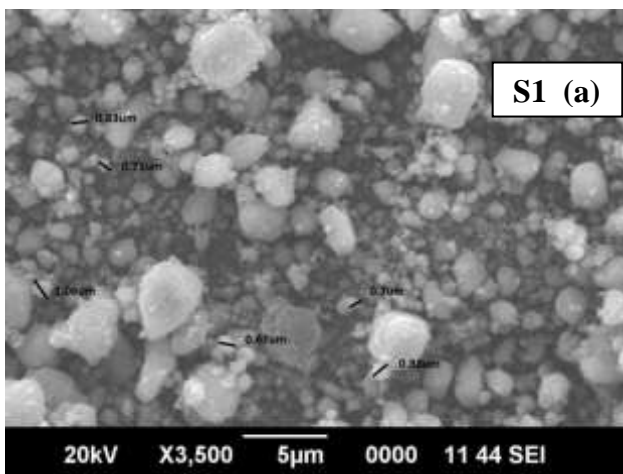


Fig3 FTIR spectra for TiO₂ nanoparticles - samples S1, S2 and S3.



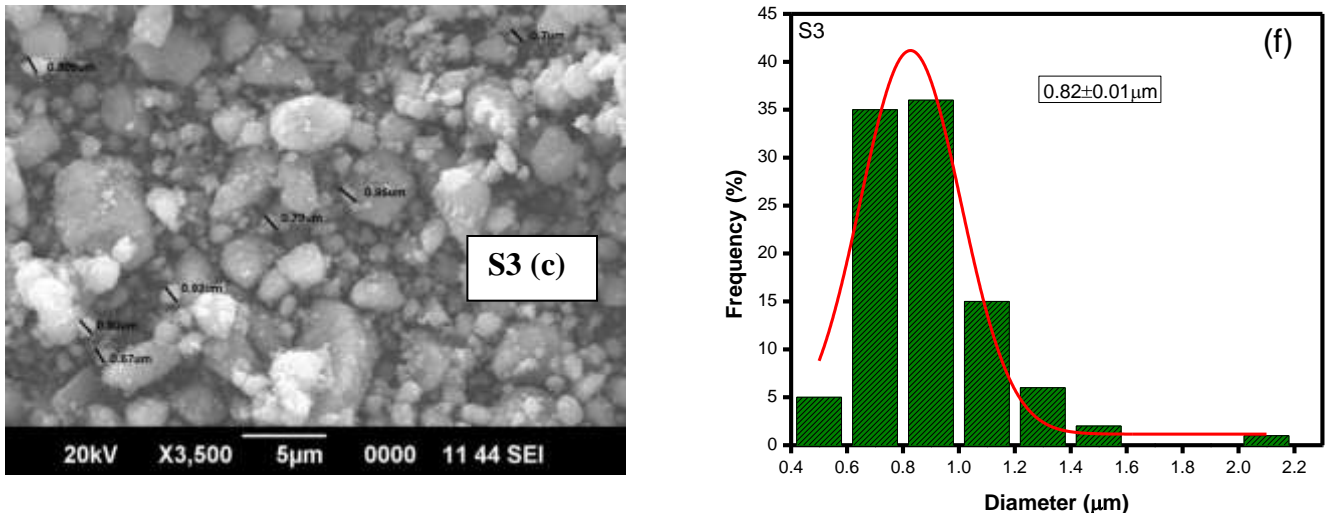


Fig 4 SEM (a,b and c) and histogram(d,e and f) images of the samples S1, S2 and S3 respectively

Morphological analysis

Scanning electron microscopy (SEM) was carried out to estimate the surface morphology of the samples. Figures 4 (a-c) shows, the SEM images of samples S1, S2 and S3 respectively and their corresponding histograms are shown in Figures 4(d-f). The SEM images revealed that the synthesized samples are spherical in shape with distribution of sizes and agglomerated [15]. We observed a slight morphological change among the samples of S1, S2 and S3 due to the different reaction times. From the SEM images, we found the average particle size of the TiO₂ samples S1, S2 and S3 are 0.76 µm, 0.776 µm and 0.825 µm respectively. Similarly from the histogram images, the average particle size distributions of samples S1, S2 and S3 are 0.74 ± 0.02 µm, 0.77 ± 0.01 µm, 0.82 ± 0.01 µm respectively [16].

UV-vis-NIR diffuse reflectance spectroscopy

Diffuse reflectance spectroscopy was used to identify the optical properties of TiO₂ nanoparticles in the wavelength range of 190-900 nm. The bandgap energy of synthesized TiO₂ nanoparticles can be estimated from the Kubelka-Munk plot of $h\nu$ vs. $[F(R) h\nu]^{1/2}$ as shown in Figure 5. The reflectance data was converted to the absorption coefficient $F(R)$ values according to the Kubelka-Munk equation [13]. The bandgap energy of three TiO₂ samples was calculated from the expression,

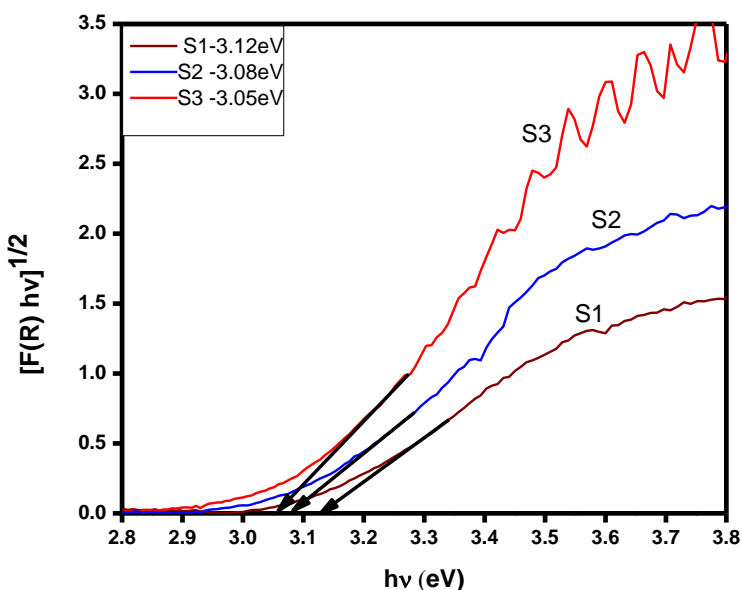


Fig5 Kubelka Munk plot : Bandgap values of three synthesized TiO₂ samples

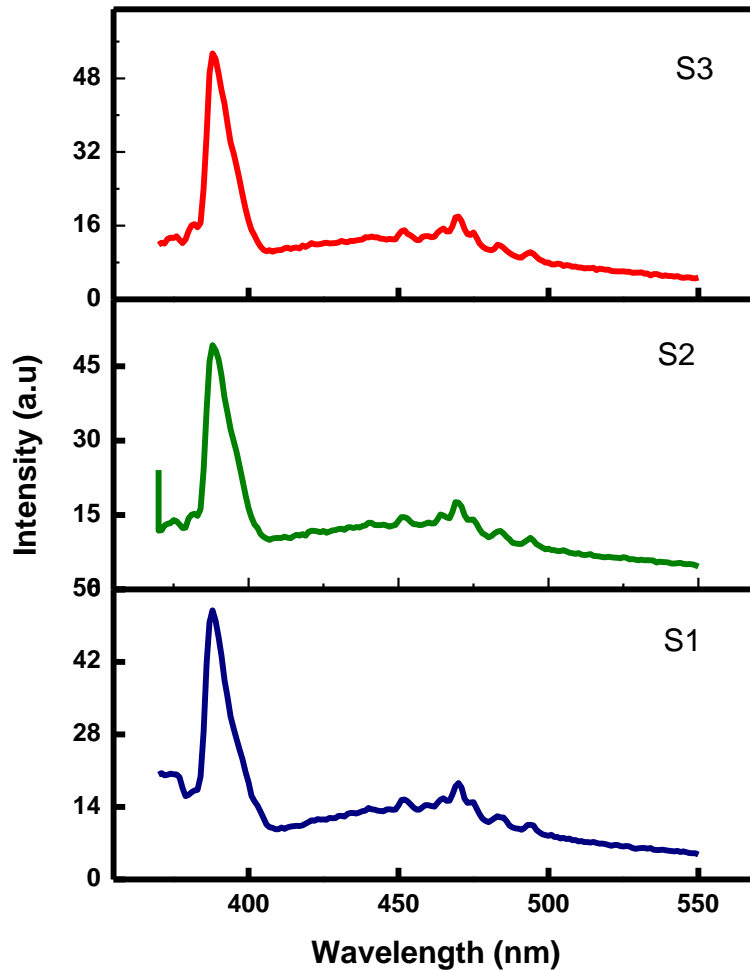


Fig 6 PL spectra of three synthesized samples of TiO₂

$$[F(R) = (1-R^2) / 2R]$$

where R is the reflectance of the samples, h is the Planck's constant and ν is the frequency of incident photon. The calculated bandgap energy values of S1, S2 and S3 samples are found to be 3.12eV, 3.08 eV and 3.05eV respectively. The particle sizes are increased with respect to the increase in reaction time but the bandgap energy decreases with the increase in particle size. This can be understood from the fact that the bandgap of semiconductors are particle size dependent [14,15]. These outcomes are well correlated with the SEM results.

Photoluminescence Spectroscopy

Photoluminescence (PL) is a practical method for inquiring the electronic structure of nanomaterials, the transfer behavior of photoexcited electron-hole pairs in semiconductors and recombination rate [16]. Figure 6 shows that the PL spectra of TiO₂ samples. The excitation wavelength is fixed as 356 nm. All the samples are exhibiting a similar kind of emission spectrum. The high intense peak at 388 nm can be ascribed to the emission of bandgap transition related to the anatase phase of TiO₂, whereas the low intense peaks at around 470 nm originates from the charge recombination at the shallow trap surface state. The existence of emission peaks in the visible region is due to the presence of defect levels below the conduction band. Basically TiO₂ consists of four types of defects: Ti interstitial (Ti_i), Titanium vacancy (V_{Ti}), oxygen interstitial (O_i) and oxygen vacancy (V_o). All of them have low formation energies under different growth conditions [17]. As the temperature increases, the structural transformations take place because of the induced oxygen vacancies and thus creating the defects level in depth and hence reducing the bandgap (red-shift) for the samples calcinated at higher temperature. The PL intensity increases when tensile strain changes in to compressive strain for samples prepared at higher temperature [19]. The recombination rate of photo generated electron and hole is directly proportional to the intensity of the PL emission. The influence of reaction time is revealed from the variation of

intensity of the PL peaks. As the reaction time increases the intensity of the PL peaks decreases and thus the rate of recombination decreases.

Conclusions

TiO₂ nanoparticles were synthesized by low temperature sol-gel method with different reaction time and various precursor concentrations. XRD analysis confirmed the formation of anatase and brookite phases. Williamson-Hall plot confirmed the compressive strain present in all the three samples. FTIR analysis confirmed the functional groups of TiO₂ nanoparticles. The SEM analysis revealed the average particle size of the synthesized S1, S2, and S3 samples of TiO₂ to be $0.74 \pm 0.02 \mu\text{m}$, $0.77 \pm 0.01 \mu\text{m}$, $0.82 \pm 0.01 \mu\text{m}$ respectively. SEM images showed that all the samples consist of agglomerated particles and larger particle size. In the present work, we got microsize range TiO₂ particles which is mainly due to calcination temperature. From UV analysis, we found the bandgap values of the synthesized TiO₂ nanoparticles. Calculated band gap energy from the Kubelka-Munk function was found to be 3.12 eV, 3.08 eV and 3.05 eV (lesser than the bulk TiO₂ bandgap value). The results of PL spectroscopy revealed that the increase of reaction time cause the reduction in the intensity of the PL peaks. Thus the increase in reaction time reduces the rate of recombination. In this work, reaction time and the concentration of the precursor play the chief roles in the structure and the morphology of the particles. The synthesized TiO₂ structure is suitable to apply in surface reaction devices such as solar cell and photochromic devices and photocatalytic applications.

References

1. Muniz E C, Goes M S, Silva J J, Varela J A, Joannib E, Parra R, et al., Synthesis and characterization of mesoporous TiO₂ nanostructured films prepared by a modified sol-gel method for application in dye solar cells, *Ceram. Int.*, 2011, 37, 1017.
2. Tasbihi M, Stangar U K, Cernigoj U and Kogej K, Low-temperature synthesis and characterization of anatase TiO₂ powders from inorganic precursors, *Photochem. Photobiol. Sci.*, 2009, 8, 719–725.
3. Mital G S, Manoj T, A review of TiO₂ nanoparticles., *Chin. Sci. Bull.*, 2011, 56, 1639.
4. Zheng Y, Shi E, Cui S, Li W and Hu X, *J. Am. Ceram. Soc.*, 2000, 83, 2634.
5. Šćepanović M, Abramović B, Golubović A, Kler S, Grujić-Brojčin M, et al., Photocatalytic degradation of metoprolol in water suspension of TiO₂ nanopowders prepared using sol-gel route *J. Sol-Gel Sci. Technol.*, 2012, 61, 390.
6. Bishel O S, Zhao F, Darvishi A R, Khodadad E R, Huang Y, Precursor and Reaction Time Effects in Evaluation of Photocatalytic Properties of TiO₂ Nanoparticles Synthesized via Low Temperature, *Int. J. Electrochem. Sci.*, 2014, 9, 3068.
7. Qin W, Szpunar J A, Origin of lattice strain in nanocrystalline materials, *Phil Mag Lett.*, 2005, 85, 649.
8. Choudhury B, Choudhury A, Local structure modification and phase transformation of TiO₂ nanoparticles initiated by oxygen defects, grain size, and annealing temperature *International Nano Letters*, 2013, 55, 1.
9. Ba-Abbad, M M, et al, Synthesis and catalytic activity of TiO₂ nanoparticles for photochemical oxidation of concentrated chlorophenols under direct solar radiation., *Int J Electrochem.*, 2012, 7, 4871.
10. Praveen P, Viruthagiri G, Mugunthan S, Shanmugam N, Structural, optical and morphological analyses of pristine titanium di-oxide nanoparticles – Synthesized via sol-gel route, *Spectrochim. Acta Mol. Biomol. Spectrosc.*, 2014, 117, 622.
11. Han Y, Kim H S, Kim H, Relationship between Synthesis Conditions and Photocatalytic Activity of Nanocrystalline TiO₂, *J. Nanomater.*, 2012, 3, 1.
12. Karthick S N, Hemalatha K V, Justin Raj C, Kim H J, Yi M, J. Titanium dioxide paste preparation for dye sensitized solar cell using hydrothermal technique *Ceram. Process Res.*, 2012, 13, s136.
13. Deiana C, Fois E, Coluccia S, Martra G, Surface structure of P25 TiO₂ nanoparticles : Infrared study of Hydroxy groups on coordinative defect sites, *J. Phys. Chem. C*, 2010, 114, 21531.
14. Karkare M M, Choice of precursor not affecting the size of anatase TiO₂ nanoparticles but affecting morphology under broader view *Int Nano Lett*, 2014, 111, 1.
15. Keiteb A S, Saion E, Zakaria A, Soltani N, Abdullahi N, A Modified Thermal Treatment Method for the Up-Scalable Synthesis of Size-Controlled Nanocrystalline Titania *Appl. Sci.*, 2016, 6, 295

16. Hong S M, Lee S, Jung H J, Yu Y, Shin J H et al., Simple Preparation of Anatase TiO₂ Nanoparticles via Pulsed Laser Ablation in Liquid, Bull. Korean Chem. Soc., 2013, 34,1279.
17. Behera D, Bag B, Sakthivel R, Relationship between Synthesis Conditions and Photocatalytic Activity of Nanocrystalline TiO₂, INDIAN J PURE & APPL PHYS, 2011, 49, 754.
18. Sabry R S, Al-Haidarie Y K, Kudhier M A, Synthesis and photocatalytic activity of TiO₂ nanoparticles prepared by sol–gel method J Sol-Gel Sci Technol, 2015, DOI 10.1007/s10971-015-3949-0
19. Tripathi A K, Singh M K, Mathpal M C , Mishra S K, Agarwal A ,study of structural transformation in TiO₂ nanoparticles and its properties, J. Alloys and Compd., 2013, 549, 119.
